Biosensors and Bioelectronics xxx (xxxx) xxx

Contents lists available at ScienceDirect

Biosensors and Bioelectronics

journal homepage: http://www.elsevier.com/locate/bios

A novel signal-off photoelectrochemical biosensor for M.SssI MTase activity assay based on GQDs@ZIF-8 polyhedra as signal quencher

Leixia Meng, Ke Xiao, Xiaohua Zhang **, Cuicui Du, Jinhua Chen *

State Key Laboratory of Chemo/Biosensing and Chemometrics, College of Chemistry and Chemical Engineering, Hunan University, Changsha, 410082, PR China

ARTICLE INFO

Keywords:
Peroxidase mimetics
GQDs
ZIF-8 polyhedra
M.SssI MTase
Signal-off
Photoelectrochemical biosensor

ABSTRACT

DNA methylation catalyzed by M.SssI methyltransferases (MTase) has important roles in gene expression and other cellular activities, and relates to some diseases, especially cancers. Therefore, it is important to develop a sensitive sensing platform for M.SssI MTase activity assay. Here, taking zeolitic imidazolate framework-8 (ZIF-8) polyhedra as the carriers of graphene quantum dots (GQDs), GQDs-embedded ZIF-8 polyhedra (denoted as GQDs@ZIF-8 polyhedra) were successfully prepared and used as the multi-functional signal quencher to construct a novel signal-off photoelectrochemical (PEC) biosensor for M.SssI MTase activity assay. Firstly, the indium tin oxide (ITO) slice was modified with TiO_2, poly(diallyldimethylammonium chloride) and CdTe quantum dots (QDs). The obtained electrode was used as the photoelectrode and labeled as ITO/TiO_2/CdTe QDs. Then, single-stranded DNA (S1) was anchored on the photoelectrode surface via S–Cd bond. After hybridization between S1 and biotinylated single-stranded DNA (S2), the streptavidin (SA)-labeled GQDs@ZIF-8 polyhedra were introduced to the modified electrode via the specific reaction between biotin and SA. As the signal quencher, GQDs@ZIF-8 polyhedra could not only inhibit the photocurrent signal of the ITO/TiO_2/CdTe QDs electrode due to the steric hindrance effect, but also act as peroxidase mimetics to catalyze precipitation reaction of 4-chloro-1-naphthol, resulting in the evident depression of the photocurrent signal. For the specially designed S1/S2 double-strand DNA, the decreased photocurrent was quantitatively correlated with the M.SssI MTase activity (linear response range, 0.005–150 U mL^{-1}; detection limit, 0.004 U mL^{-1}). The developed GQDs@ZIF-8 polyhedra and related PEC biosensor may have potential applications in clinical research and disease diagnosis.

1. Introduction

DNA methylation is a significant epigenetic event, which takes place in various biological activities, including genomic imprinting, cell proliferation, gene expression and gene transcription (Law et al., 2010; Reik et al., 2001). DNA methyltransferase (MTase) can serve as a kind of catalyst to catalyze the DNA methylation via transferring a $–CH_3$ group from S-adenosyl-$_L$-methionine (SAM) to cytosine or adenine (Hou et al., 2019). Aberrant DNA methylation associates with a variety of cancers, for instance, ovarian cancer (Bondurant et al., 2011), gastric cancer (Mutze et al., 2011), breast cancer (Szyf et al., 2012) and lung cancer (Belinsky et al., 1996). At present, a number of techniques have been reported for DNA MTase activity determination, including high-performance liquid chromatography (HPLC) (Wenzel and Guschlbauer, 1993), polymerase chain reaction (PCR) (Van Steensel et al., 2000), electrochemiluminescence (ECL) (Zhou et al., 2016), and gel electrophoresis (Rebeck et al., 1991). However, most of them suffer from expensive equipments, complex operation process, and professional technicians, which makes them have challenge for DNA MTase activity assay.

Recently, photoelectrochemical (PEC) biosensor, as a newly emerging and promising method, has attracted profound attention owing to the advantages of simplicity, economy, miniaturization and low background signal (Zhao et al., 2014). Compared with the conventional methods, it displays superior properties due to the total separation of the incident light source and output photocurrent signal (Hu et al., 2018; Li et al., 2014; Wang et al., 2018). As one of the typical PEC sensing modes, signal-off methods have been widely developed based on different quenching strategies, such as steric hindrance effect, resonance energy transfer effect, precipitation effect and so on (Zhang et al., 2019; Zhao et al., 2012, 2015). However, only a few signal-off PEC biosensors have been reported to determine DNA MTase activity (Shen et al., 2015;

* Corresponding author.
** Corresponding author.
E-mail addresses: mickyxie@hnu.edu.cn (X. Zhang), chenjinhua@hnu.edu.cn (J. Chen).

https://doi.org/10.1016/j.bios.2019.111861
Received 26 August 2019; Received in revised form 6 November 2019; Accepted 7 November 2019
Available online 11 November 2019

Zhou et al., 2014). For instance, Zhou et al. reported a PEC biosensor for DNA MTase activity assay based on steric hindrance effect of methyl binding domain protein (Zhou et al., 2014). Shen et al. proposed a PEC sensing platform to determine DNA MTase activity via resonance energy transfer effect of Au nanoparticles (NPs) (Shen et al., 2015). However, these signal quenchers involve complicated protein expression, high-cost metal and sophisticated labeling process. Therefore, it is desired to develop an easy-preparation, cheap and effective signal quencher for the construction of PEC biosensor and DNA MTase activity assay.

Graphene quantum dots (GQDs) with a size of several nanometers and a constitution of single or few-layer graphenes (Pan et al., 2010; Xu et al., 2015; Zou et al., 2016) have received enormous interest owing to their characteristics of low cost, good biocompatibility, low cytotoxicity, rich functional groups and so on (Deng et al., 2017; Fan et al., 2018; Pang et al., 2016). GQDs have been found to possess intrinsic peroxidase-like activity to catalyze the oxidation of 3,3′,5,5′-tetramethylbenzidine (TMB) with the aid of H_2O_2 (Li et al., 2016; Sun et al., 2014). On the other hand, as a kind of zeolitic imidazolate framework (ZIF), ZIF-8 polyhedra have numerous merits, including high surface area, biocompatibility, superior chemical and thermal stability (Wang et al., 2019; Zheng et al., 2016; Zhu et al., 2018), and are widely used as carriers for metal NPs (Chizallet et al., 2010), drugs (Sun et al., 2012), enzymes (Ma et al., 2013), semiconductors (Fu et al., 2018) and so on. Additionally, ZIF-8 polyhedra have poor electric conductivity (Wang et al., 2019). These imply that ZIF-8 polyhedra may be utilized as carriers and signal inhibitors in PEC sensing system.

The above attractive advantages of GQDs and ZIF-8 polyhedra inspire us to develop the GQDs-embedded ZIF-8 polyhedra (denoted as GQDs@ZIF-8 polyhedra) as the multi-functional signal quencher to construct a signal-off PEC biosensor for DNA MTase activity assay (Scheme 1). Firstly, the indium tin oxide (ITO) slice was modified with TiO_2, poly(diallyldimethylammonium chloride) (PDDA) and CdTe quantum dots (QDs). The obtained electrode was used as the photoelectrode (labeled as ITO/TiO_2/CdTe QDs). Then, single-stranded DNA (S1) was anchored on the photoelectrode surface via S–Cd bond. After hybridization between S1 and biotinylated single-stranded DNA (S2), the streptavidin (SA)-labeled GQDs@ZIF-8 polyhedra were introduced to the modified electrode via the specific reaction between biotin and SA. Here, as the signal quencher, GQDs@ZIF-8 polyhedra could not only inhibit the photocurrent signal of the ITO/TiO_2/CdTe QDs electrode due to the steric hindrance effect, but also act as peroxidase mimetics to catalyze precipitation reaction of 4-chloro-1-naphthol (4-CN), resulting in the evident depression of the photocurrent signal. For the specially designed S1/S2 double-strand DNA (ds-DNA), the decreased photocurrent was quantitatively correlated with the M.SssI MTase activity (wide linear range, 0.005–150 U mL^{-1}; low detection limit, 0.004 U mL^{-1}). The prepared GQDs@ZIF-8 polyhedra and related PEC biosensor may have potential applications in clinical research and disease diagnosis.

2. Experimental section

2.1. Reagents, apparatus and materials preparation

The reagents and apparatus used in this work are detailed in Supplementary material. The procedures for the preparation of CdTe QDs, GQDs, GQDs@ZIF-8 polyhedra and SA-labeled GQDs@ZIF-8 polyhedra (GQDs@ZIF-8-SA) are also described in Supplementary material.

2.2. Preparation of the PEC biosensor and M.SssI MTase activity assay

The preparation process of the ITO/TiO_2/CdTe QDs electrode is described in Supplementary material. For the establishment of the PEC biosensor and M.SssI MTase activity assay, the prepared ITO/TiO_2/CdTe

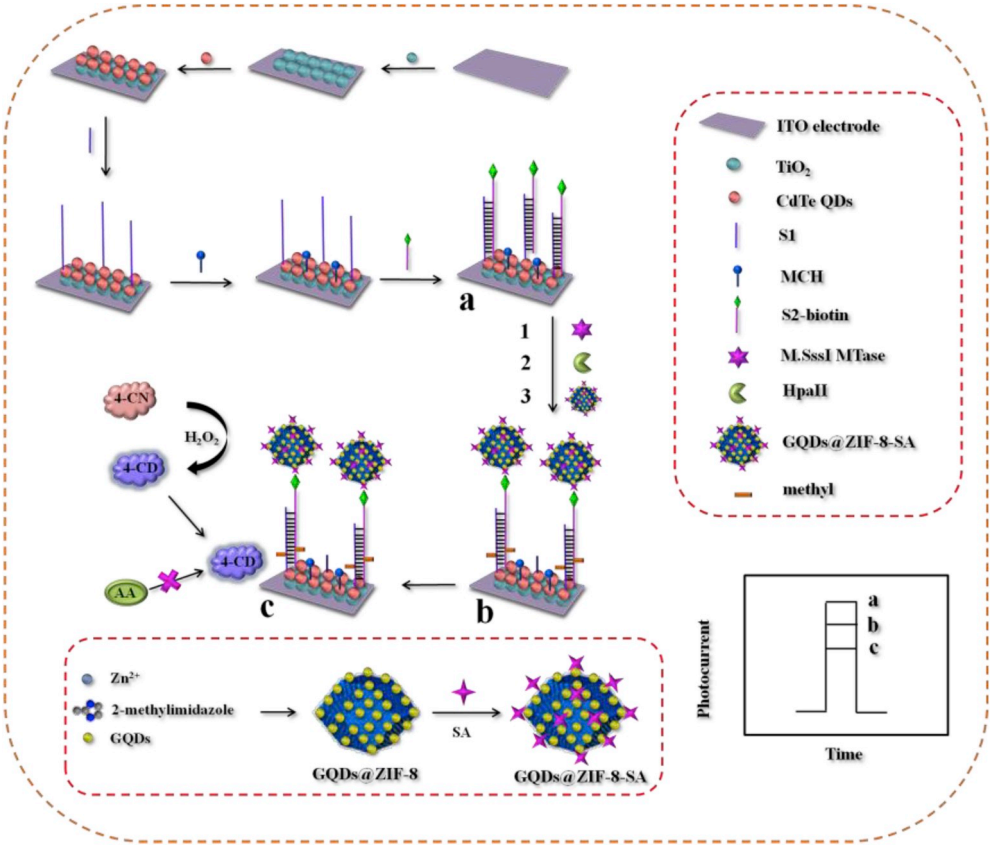

Scheme 1. Preparation process of the developed signal-off PEC biosensor to detect M.SssI MTase activity based on GQDs@ZIF-8 polyhedra as signal quencher.

QDs electrode was modified with thiolated S1 via the Cd–S bond. Before the assembly of S1 on the above modified electrode, S1 was prepared in 10 mM Tris-HCl buffer (0.1M NaCl, 10 mM Tris-(2-carboxyethyl) phosphine hydrochloride (TCEP), pH 7.4), and incubated for 1 h to decrease disulfide bonds. Afterwards, 20 μL of 1 μM S1 was dripped on the ITO/TiO_2/CdTe QDs electrode at 4 °C for 16 h to immobilize S1 on the electrode via the Cd–S bond, followed by washing with 10 mM Tris-HCl (pH 7.4). To avoid the nonspecific adsorption, 20 μL of 2 mM 6-mercaptohexanol (MCH) was coated on the electrode for 1 h at room temperature, and then the electrode was washed with 10 mM Tris-HCl (pH 7.4). After that, the electrode was incubated with 20 μL of 1 μM S2 dissolved in 10 mM Tris-HCl (0.1 M NaCl, 0.02M $MgCl_2$, pH 7.4) at 37 °C for 2 h, and then rinsed with 10 mM Tris-HCl (pH 7.4).

Subsequently, the modified electrode was incubated with 20 μL of the 1 × NEBuffer 2 containing various concentrations of M.SssI MTase and 160 μM SAM at 37 °C for 2 h to carry out the methylation at the CpG sites of the immobilized ds-DNA, then rinsed with 10 mM Tris-HCl (pH 7.4). The electrode was incubated with 20 μL of the 1 × CutSmart buffer containing 50 U mL^{-1} HpaII restriction endonuclease which can recognize the CpG sites to digest the unmethylated ds-DNA at 37 °C for 2 h. After washed thoroughly with 10 mM Tris-HCl (pH 7.4), the electrode was incubated with 20 μL of the prepared GQDs@ZIF-8-SA solution at 37 °C for 2 h to introduce GQDs@ZIF-8-SA to the electrode surface via the specific reaction between biotin and SA, followed by rinsing with 10 mM Tris-HCl (pH 7.4) to remove the unbound GQDs@ZIF-8-SA. Finally, the electrode was incubated with 5 mM 4-CN containing 1 mM H_2O_2 for 25 min at ambient temperature and washed with 10 mM Tris-HCl (pH 7.4). PEC measurement of the resulting electrode was carried out in 0.1 M phosphate buffer solution (PBS, pH 7.4) containing 0.1M ascorbic acid (AA) at 0 V.

3. Results and discussion

3.1. Characterization of ITO/TiO_2/CdTe QDs electrode

The morphologies of the bare ITO, ITO/TiO_2, and ITO/TiO_2/CdTe QDs electrodes were characterized by scanning electron microscopy (SEM) (Fig. 1). In comparison with the bare ITO electrode (Fig. 1A), many TiO_2 NPs are modified on the electrode surface (Fig. 1B) and the average size of TiO_2 NPs is about 20 nm according to the transmission electron microscopy (TEM) image (Fig. S1A, see Supplementary material section). From Fig. S1B (see Supplementary material section), it is noted that the average size of the as-prepared CdTe QDs is about 3.80 nm and a lattice distance of 0.37 nm should relate to the (111) facet of CdTe QDs. After CdTe QDs are coated on the ITO/TiO_2 electrode with the assistance of PDDA (Fig. 1C), the morphology of the electrode is changed. Furthermore, three elements (Ti, Cd, and Te) exist on the electrode and are uniformly distributed (Fig. S2, see Supplementary material section), indicating that the ITO/TiO_2/CdTe QDs electrode is successfully prepared.

3.2. Characterization of GQDs@ZIF-8 polyhedra

The obtained GQDs were investigated by TEM and atomic force microscopy (AFM). From Fig. S3A (see Supplementary material section), GQDs are homogeneous particles with an average size of 4.14 nm. Specifically, its high-resolution TEM (HRTEM) image in insert plot shows that the lattice distance of 0.24 nm is matched well with the (1120) facet of graphene. The AFM image (Fig. S3B, see Supplementary material section) displays that the average height of the GQDs is 1.28 nm, demonstrating that the GQDs are mainly bi-layered (Zeng et al., 2016).

The as-prepared polyhedra (ZIF-8 and GQDs@ZIF-8) were also characterized. As shown in Fig. 2A, ZIF-8 polyhedra have the typical rhombic dodecahedron morphology with a mean size of about 115 nm. This morphology is also observed in the previous works (Gai et al., 2013; Jiang et al., 2012). For the GQDs@ZIF-8 polyhedra, they retain the similar morphology of ZIF-8 polyhedra, while the average size of the GQDs@ZIF-8 polyhedra (about 90 nm, Fig. 2B) is smaller than that of the ZIF-8 polyhedra, illustrating that GQDs may affect the formation of ZIF-8 polyhedra. These materials are further evaluated by the HRTEM (Fig. 2C and D). Compared with ZIF-8 polyhedra (Fig. 2C), GQDs@ZIF-8 polyhedra (Fig. 2D) exhibit the lattice spacing of 0.24 nm, which is in agreement with the above HRTEM result of GQDs (Fig. S3A, see Supplementary material section), suggesting that GQDs are successfully encapsulated in ZIF-8 polyhedra and the GQDs@ZIF-8 polyhedra have been prepared according to Scheme 1.

3.3. EIS and PEC characterization of the constructed PEC biosensor

Electrochemical impedance spectroscopy (EIS) is an excellent method for monitoring the stepwise preparation process of the electrode. Typically, the semicircular diameter at a high frequency reflects the change of the interface electron transfer resistance (R_{ct}). The EIS results of different electrodes are shown in Fig. 3A. From Fig. 3A, the values of R_{ct} are obtained according to Randles equivalent circuit model (Fig. S4, see Supplementary material section) and shown in Table S1 (see Supplementary material section). It is noted that the bare ITO electrode exhibits a small R_{ct} value (curve a), demonstrating rapid charge transfer process of redox probe at the electrode surface. After modification of TiO_2 (curve b) and CdTe QDs (curve c) on the ITO electrode, R_{ct} values increase, which is attributed to the semiconductor properties of TiO_2 and CdTe QDs, and the low electric conductivity of the PDDA polymer. After that, the stepwise modification of S1, MCH and S2 results in the successive increase of R_{ct} value (curves d to f), which should be ascribed to the poor charge transfer properties of oligonucleotides and organic molecules and the repulse effect between the negative-charged DNA strands and anions ($Fe(CN)_6^{3-/4-}$). After the incubation of M.SssI MTase and HpaII, the GQDs@ZIF-8-SA were introduced to the electrode via the specific reaction between biotin and SA (curve g), the R_{ct} value of the electrode further increases because GQDs@ZIF-8 polyhedra with the poor electric conductivity and large size hinder the movement of redox probe to the electrode interface. When the above electrode is further incubated with 5 mM 4-CN solution containing 1 mM H_2O_2, the R_{ct} value of the electrode sharply increases (curve h). The reason should be as follows: in the presence of H_2O_2, GQDs act as peroxidase mimetics to catalyze the generation of benzo-4-chlorohexadienone (4-CD) from 4-chloro-1-naphthol (4-CN), and the insoluble precipitate 4-CD

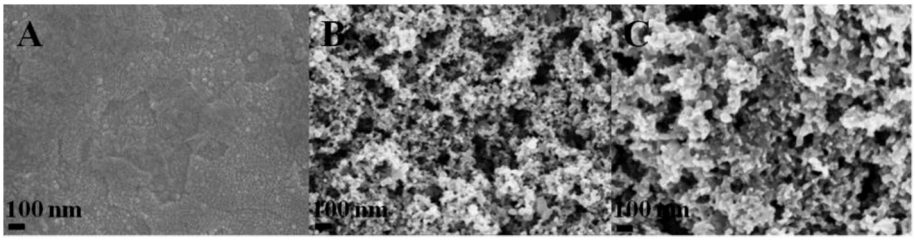

Fig. 1. SEM images of (A) bare ITO, (B) ITO/TiO_2 and (C) ITO/TiO_2/CdTe QDs electrodes.

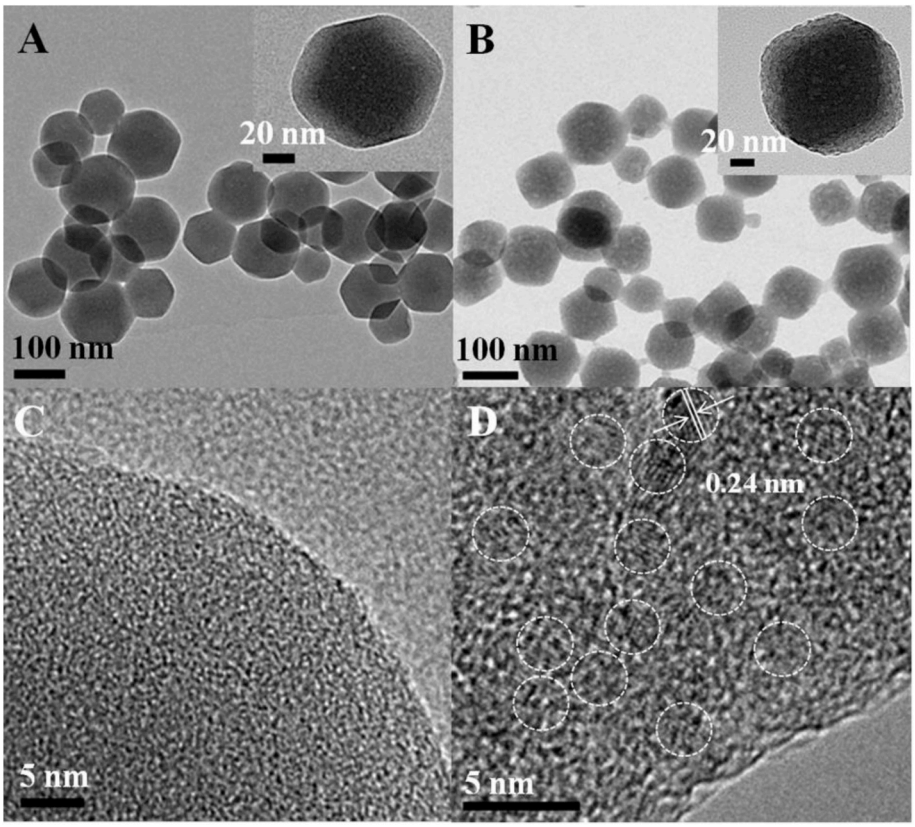

Fig. 2. TEM images of (A) ZIF-8 and (B) GQDs@ZIF-8 polyhedra. HRTEM image of (C) ZIF-8 and (D) GQDs@ZIF-8 polyhedra.

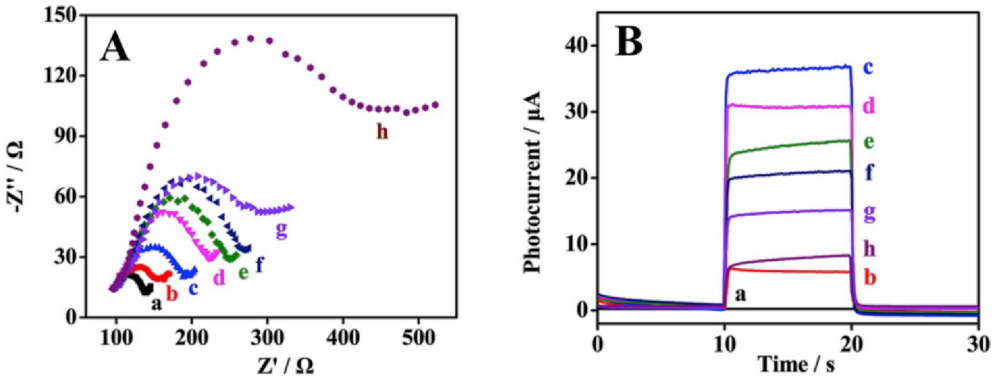

Fig. 3. (A) EIS results of the different photoelectrodes in 0.1 M KCl aqueous solution containing 5 mM $[Fe(CN)_6]^{3-}$ and 5 mM $[Fe(CN)_6]^{4-}$. Frequency, 0.01 Hz −100 kHz; amplitude, 5 mV. (B) PEC results of the different electrodes in 0.1 M PBS (pH 7.4) containing 0.1 M AA at 0 V. (a) bare ITO, (b) ITO/TiO_2, (c) ITO/TiO_2/CdTe QDs, (d) ITO/TiO_2/CdTe QDs/S1, (e) ITO/TiO_2/CdTe QDs/S1/MCH, (f) ITO/TiO_2/CdTe QDs/S1/MCH/S2, (g) ITO/TiO_2/CdTe QDs/S1/MCH/S2 electrode incubated with M.SssI MTase/HpaII/GQDs@ZIF-8-SA, (h) ITO/TiO_2/CdTe QDs/S1/MCH/S2 electrode incubated with M.SssI MTase/HpaII/GQDs@ZIF-8-SA/4-CN containing H_2O_2. M.SssI MTase, 50 U mL^{-1}; HpaII, 50 U mL^{-1}.

accumulates on the electrode surface, leading to the obstacle of the electron transfer of redox probe at the electrode surface. Here, it is the first time to utilize GQDs as peroxidase mimic to catalyze the precipitation reaction of 4-CN to detect M.SssI MTase activity with PEC method. The possible mechanism for the generation of 4-CD from 4-CN is as follows: H_2O_2 is catalyzed by GQDs@ZIF-8 polyhedra to produce hydroxyl radical (·OH) and the resultant.OH reacts with 4-CN to form the insoluble 4-CD which accumulates on the electrode (Hassanzadeh et al., 2018; Li et al., 2016; Liu et al., 2014; Sun et al., 2014). The above EIS results reveal that the modification process of the electrode is successfully carried out according to Scheme 1.

The construction process of the proposed PEC biosensor was also characterized by PEC measurement (Fig. 3B). The bare ITO has no obvious photocurrent signal (curve a). As expected, an anodic photocurrent is observed for the ITO/TiO_2 electrode due to the good photoelectric properties of TiO_2 (curve b). Compared with the ITO/TiO_2 electrode (curve b), the ITO/TiO_2/CdTe QDs electrode shows an obviously enhanced anodic photocurrent (curve c) because of the sensitization effect of CdTe QDs based on the matched energy levels between TiO_2 and CdTe QDs (Fan et al., 2014), which is beneficial to improving the analytical performance of the signal-off PEC biosensor. When the above electrode is successively modified with S1, MCH and S2, the photocurrent of the electrode decreases in order due to the blocking effects of the DNA strands and MCH (curves d to f). After the modification of M.SssI MTase, HpaII and GQDs@ZIF-8-SA, an obvious decrease of the photocurrent can be observed (curve g). This should result from the steric hindrance effect of ZIF-8 polyhedra due to their poor electric conductivity and large size. Subsequently, a large decrease of the photocurrent is found after the above electrode is incubated with 4-CN solution containing H_2O_2 (curve h). The reason should be that the insoluble precipitate of 4-CD (Fig. S5, see Supplementary material section) is generated from 4-CN based on the peroxidase mimic property of

GQDs, and deposited on the electrode surface to inhibit the oxidation of AA, as observed in EIS result (curve h in Fig. 3A). On the other hand, ZIF-8 polyhedra are used as good carriers to load more GQDs peroxidase mimic, which further results in the decrease of the photocurrent. These results suggest that the signal-off PEC biosensor based on GQDs@ZIF-8 polyhedra as multi-functional signal quencher has been successfully established and may be utilized for the M.SssI MTase activity assay.

3.4. Optimization of experimental conditions

To obtain the good analytical performance of the developed PEC biosensor, some factors, including the amount of TiO_2, the coating number of CdTe QDs, the incubation time (t_1) of M.SssI MTase and the incubation time (t_2) of 4-CN solution, were examined.

The effect of the TiO_2 amount on the photocurrent of the ITO/TiO_2/CdTe QDs electrode was investigated. A series of TiO_2 suspensions with the same volume and different concentrations were used to prepare the electrodes. As displayed in Fig. 4A, the photocurrent of the electrode increases while the concentration of the TiO_2 suspension increases from 0.5 to 1.0 mg mL^{-1}, because more TiO_2 can offer more sites to immobilize CdTe QDs and to generate the photocurrent (Park et al., 2000). However, the photocurrent of the electrode decreases with the further increase of the TiO_2 concentration. This may result from the semiconductor properties of TiO_2. Excessive TiO_2 may inhibit the electron transfer process, resulting in the decline of the photocurrent (Kuang et al., 2006). Hence, 1.0 mg mL^{-1} is selected as the optimal concentration of TiO_2.

The coating numbers of CdTe QDs were also investigated. In Fig. 4B, with the increase of the coating numbers, the amount of CdTe QDs coated on the TiO_2 film increases, leading to the more light absorption and the increase in photocurrent signal (Chi et al., 2008). Also, excessive CdTe QDs make the photocurrent decrease, due to the semiconductor properties of CdTe QDs and the obstruction of PDDA to the diffusion of AA (Vogel et al., 1994). The results shown in Fig. 4B reveal that the optimal coating number of CdTe QDs is three.

The incubation time (t_1) of M.SssI MTase is significant for the analytical properties of the biosensor. From Fig. 4C, the photocurrent decreases with the increase of t_1 and achieves a plateau at 2 h, implying the saturation of the methylation level is achieved. Hence, 2 h is chosen as the optimal time of t_1.

The influence of incubation time (t_2) of 4-CN solution containing H_2O_2 on the photocurrent signal of the biosensor was also studied. In Fig. 4D, when the t_2 increases, the photocurrent of the biosensor decreases, because the longer incubation time results in more insoluble precipitate of 4-CD formed on the electrode interface. Further, it is observed that the photocurrent reaches a plateau at 25 min. Therefore, 25 min is served as the optimal time of t_2.

3.5. PEC assay of M.SssI MTase activity

Under the optimal experimental conditions, the developed PEC biosensor was utilized to detect M.SssI MTase activity. Because of the multi-functional signal quenching effects of GQDs@ZIF-8 polyhedra (the steric hindrance effect and peroxidase mimetics feature), the photocurrent signal of the developed PEC biosensor decreases with the increasing concentration of M.SssI MTase, as shown in Fig. 5A. A linear relationship between the photocurrent and the logarithm of M.SssI MTase concentration is obtained in the range from 0.005 to 150 U mL^{-1} (Fig. 5B). The linear equation is I (μA) = $-4.353 \log C_{MTase}$ (U mL^{-1}) + 15.22 ($R^2 = 0.9998$). The limit of detection (LOD) can be calculated to be 0.004 U mL^{-1} with the equation of LOD = $3S/k$ (S is the standard deviation of the blank signals, k is the slope of the linear equation of calibration curve (Deng et al., 2019)), which is much lower than that of recently published methods (Table S2, see Supplementary material section).

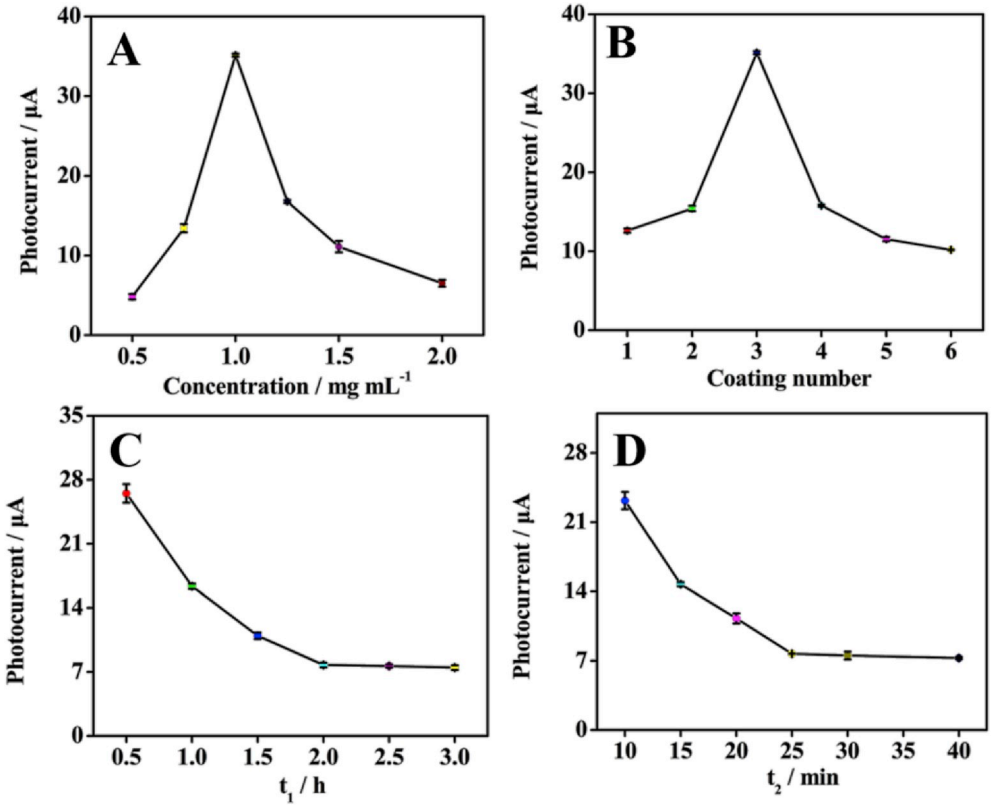

Fig. 4. Influences of the (A) concentration of TiO_2 suspension (coating number of CdTe QDs, 3) and (B) coating number of CdTe QDs (concentration of TiO_2 suspension, 1 mg mL^{-1}) on photocurrent signals of the ITO/TiO_2/CdTe QDs electrode. Effects of the (C) incubation time (t_1) of M.SssI MTase (t_2, 30 min) and (D) incubation time (t_2) of 4-CN solution containing H_2O_2 (t_1, 2h) on photocurrent signals of the biosensor. Error bars stand for the standard deviation of three independent experiments.

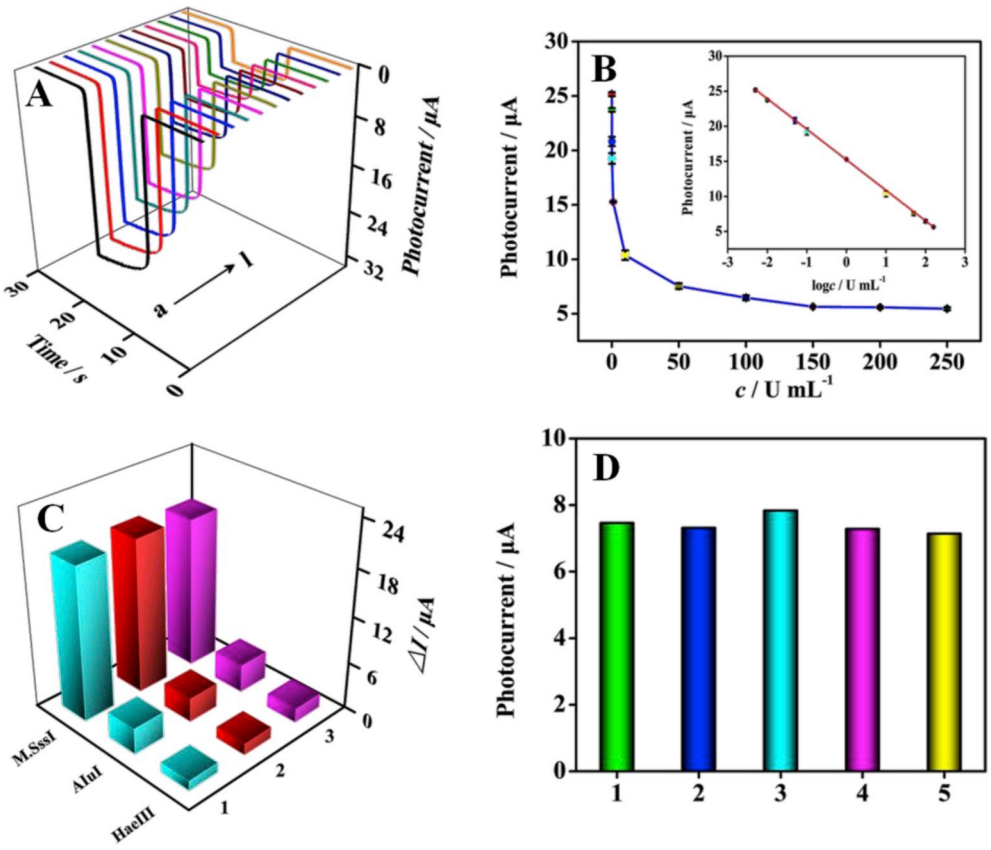

Fig. 5. (A) Photocurrent signals of the developed PEC biosensor towards different concentrations of M.SssI MTase. From a to l: 0, 0.005, 0.01, 0.05, 0.1, 1, 10, 50, 100, 150, 200 and 250 U mL^{-1}. (B) Plot of photocurrent versus the M.SssI MTase concentration. Error bars stand for the standard deviation of three independent experiments. (C) The photocurrent signals of the constructed PEC biosensor towards different MTase. AluI, 100 U mL^{-1}; HaeIII, 100 U mL^{-1}; M.SssI, 50 U mL^{-1}. (D) Reproducibility of the PEC biosensor incubated with 50 U mL^{-1} M.SssI MTase in the same batch.

3.6. Selectivity, stability and reproducibility of the constructed PEC biosensor

For the PEC biosensor, the selectivity is a crucial parameter for its potential application in complex media. To assess the selectivity of the constructed PEC biosensor, HaeIII MTase and AluI MTase were employed as the interference enzymes. As shown in Fig. 5C, the photocurrent responses ΔI ($\Delta I = I_0 - I$, I_0 and I are the photocurrent values of the established PEC biosensor in blank solution and in the solution with M.SssI MTase or interferents, respectively) towards M.SssI MTase is much larger than those towards HaeIII MTase and AluI MTase, which is attributed to that HaeIII MTase or AluI MTase cannot methylate the CpG sites. Thus, the developed PEC biosensor displays good selectivity towards M.SssI MTase.

The reproducibility of the established PEC biosensor was further explored. Five modified electrodes were utilized to detect the same concentration of M.SssI MTase (50 U mL^{-1}) under the same conditions, and the results were displayed in Fig. 5D. The relative standard deviation (RSD) of photocurrent signal is about 3.6%, giving a satisfactory reproducibility. The stability is another significant factor for the PEC biosensor. In order to investigate the stability, the ITO/TiO_2/CdTe QDs/S1/MCH/S2 electrode was kept at 4 °C for 14 days. The photocurrent signal still remains about 98.6% of the initial value for 50 U mL^{-1} M.SssI MTase, which demonstrates an acceptable stability.

3.7. Recovery test

To assess the feasibility of the constructed PEC biosensor in practical application, M.SssI MTase was spiked into the diluted human serum samples at different concentrations. From Table S3 (see Supplementary material section), the average recoveries for the added M.SssI MTase with 0.01, 0.1 and 1 U mL^{-1} are 99.3%, 103.4% and 105.5%, respectively. The results illustrate a good potentiality of the developed PEC biosensor to detect M.SssI MTase activity in real biological sample.

4. Conclusions

In summary, taking GQDs@ZIF-8 polyhedra as the multi-functional signal quencher, a novel signal-off PEC biosensor was constructed to detect M.SssI MTase activity. As the signal quencher, GQDs@ZIF-8 polyhedra can not only inhibit the photocurrent of the ITO/TiO_2/CdTe QDs electrode due to their steric hindrance effect, but also act as peroxidase mimetics to catalyze precipitation reaction of 4-CN, resulting in the obvious depression of the photocurrent signal. The designed PEC biosensor displays a wide linear response range (0.005–150 U mL^{-1}) and a low detection limit (0.004 U mL^{-1}). Furthermore, the PEC biosensor exhibits good selectivity, satisfactory reproducibility and acceptable stability. The prepared GQDs@ZIF-8 polyhedra provide a new signal quencher to establish signal-off PEC biosensors and pave a new avenue to explore other multifunctional signal quenchers.

Declaration of competing interest

The authors declare that they have no known competing financial interests or personal relationships that could have appeared to influence the work reported in this paper.

CRediT authorship contribution statement

Leixia Meng: Investigation, Methodology, Data curation, Writing - original draft. **Ke Xiao:** Data curation. **Xiaohua Zhang:** Validation, Data curation. **Cuicui Du:** Writing - review & editing. **Jinhua Chen:** Conceptualization, Supervision, Writing - review & editing.

Acknowledgements

This work was financially supported by NSFC (21727810, 21475035), and the Foundation for Innovative Research Groups of NSFC (21521063).

Appendix A. Supplementary data

Supplementary data to this article can be found online at https://doi.org/10.1016/j.bios.2019.111861.

References

Belinsky, S.A., Nikula, K.J., Baylin, S.B., Issa, J.P., 1996. Proc. Natl. Acad. Sci. U.S.A. 93, 4045–4050.
Bondurant, A.E., Huang, Z., Whitaker, R.S., Simel, L.R., Berchuck, A., Murphy, S.K., 2011. Gynecol. Oncol. 123, 581–587.
Chi, C.F., Lee, Y.L., Weng, H.S., 2008. Nanotechnology 19, 19.
Chizallet, C., Lazare, S., Bazer-Bachi, D., Bonnier, F., Lecocq, V., Soyer, E., Quoineaud, A. A., Bats, N., 2010. J. Am. Chem. Soc. 132, 12365–12377.
Deng, H.M., Huang, L.J., Chai, Y.Q., Yuan, R., Yuan, Y.L., 2019. Anal. Chem. 91, 2861–2868.
Deng, Y.C., Tang, L., Feng, C.Y., Zeng, G.G., Wang, J.J., Lu, Y., Liu, Y.N., Yu, J.F., Chen, S., Zhou, Y.Y., 2017. ACS Appl. Mater. Interfaces 9, 42816–42828.
Fan, D.W., Bao, C.Z., Khan, M.S., Wang, C.L., Zhang, Y., Liu, Q.Z., Zhang, X., Wei, Q., 2018. Biosens. Bioelectron. 106, 14–20.
Fan, G.C., Han, L., Zhang, J.R., Zhu, J.J., 2014. Anal. Chem. 86, 10877–10884.
Fu, X., Li, H., Lv, R., Hong, D., Yang, B.Y., Gu, W., Liu, X., 2018. J. Solid State Chem. 264, 35–41.
Gai, P.B., Zhang, H.J., Zhang, Y.S., Liu, W., Zhu, G.B., Zhang, X.H., Chen, J.H., 2013. J. Mater. Chem. B 1, 2742−274.
Hassanzadeh, J., Khataee, A., 2018. Talanta 178, 992–1000.
Hou, T., Xu, N.N., Wang, W.X., Ge, L., Li, F., 2019. Biosens. Bioelectron. 141, 111395.
Hu, T., Zheng, Y.N., Li, M.J., Liang, W.B., Chai, Y.Q., Yuan, R., 2018. Anal. Chem. 90, 6096–6101.
Jiang, Z., Sun, H.Y., Qin, Z.H., Jiao, X.L., Chen, D.R., 2012. Chem. Commun. 48, 3620–3622.
Kuang, D.B., Ito, S., Wenger, B., Klein, C., Moser, J.E., Humphry-Baker, R., Zakeeruddin, S.M., Gratzel, M., 2006. J. Am. Chem. Soc. 128, 4146–4154.
Law, J.A., Jacobsen, S.E., 2010. Nat. Rev. Genet. 11, 204–220.
Li, N., Than, A., Wang, X.W., Xu, S.H., Sun, L., Duan, H.W., Xu, C.J., Chen, P., 2016. ACS Nano 10, 3622–3629.
Li, R.Z., Liu, Y., Cheng, L., Yang, C.Z., Zhang, J.D., 2014. Anal. Chem. 86, 9372–9375.
Liu, W.Y., Yang, H.M., Ma, C., Ding, Y.N., Ge, S.G., Yu, J.H., Yan, M., 2014. Anal. Chim. Acta 852, 181–188.
Ma, W.J., Jiang, Q., Yu, P., Yang, L.F., Mao, L.Q., 2013. Anal. Chem. 85, 7550–7557.
Mutze, K., Langer, R., Schumacher, F., Becker, K., Ott, K., Novotny, A., Hapfelmeier, A., Höfler, H., Keller, G., 2011. Eur. J. Cancer 47, 1817–1825.
Pan, D.Y., Zhang, J.C., Li, Z., Wu, M.H., 2010. Adv. Mater. 22, 734–738.
Pang, X.H., Zhang, Y., Liu, C., Huang, Y., Wang, Y.G., Pan, J.H., Wei, Q., Du, B., 2016. J. Mater. Chem. B 4, 4612–4619.
Park, N.G., van de Lagemaat, J., Frank, A.J., 2000. J. Phys. Chem. B 104, 8989–8994.
Rebeck, G.W., Samson, L.J., 1991. J. Bacteriol. 173, 2068–2076.
Reik, W., Dean, W., Walter, J., 2001. Science 293, 1089–1093.
Shen, Q.M., Han, L., Fan, G.C., Abdel-Halim, E.S., Jiang, L.P., Zhu, J.J., 2015. Biosens. Bioelectron. 64, 449–455.
Sun, C.Y., Qin, C., Wang, X.L., Yang, G.S., Shao, K.Z., Lan, Y.Q., Su, Z.M., Huang, P., Wang, C.G., Wang, E.B., 2012. Dalton Trans. 41, 6906–6909.
Sun, H.J., Gao, N., Dong, K., Ren, J.S., Qu, X.G., 2014. ACS Nano 8, 6202–6210.
Szyf, M., 2012. Genome Med. 4, 26.
Van Steensel, B., Henikoff, S., 2000. Nat. Biotechnol. 18, 424–428.
Vogel, R., Hoyer, P., Weller, H., 1994. J. Phys. Chem. 98, 3183–3188.
Wang, H.Q., Ma, Z.F., 2019. Biosens. Bioelectron. 132, 265–270.
Wang, Z.Y., Liu, J., Liu, X., Shi, X.Y., Dai, Z.H., 2018. Anal. Chem. 91, 830–835.
Wenzel, C., Guschlbauer, W., 1993. Nucleic Acids Res. 21, 4604–4609.
Xu, C.Y., Han, Q., Zhao, Y., Wang, L.X., Li, Y., Qu, L.T., 2015. J. Mater. Chem. A 3, 1841–1846.
Zeng, Z.P., Xiao, F.X., Gui, X.C., Wang, R., Liu, B., Yang Tan Yang, T., 2016. J. Mater. Chem. A 4, 16383–16393.
Zhang, L., Shi, X.M., Xu, Y.T., Fan, G.C., Yu, X.D., Liang, Y.Y., Zhao, W.W., 2019. Biosens. Bioelectron. 134, 103–108.
Zhao, M., Fan, G.C., Chen, J.J., Shi, J.J., Zhu, J.J., 2015. Anal. Chem. 87, 12340–12347.
Zhao, W.W., Xu, J.J., Chen, H.Y., 2014. Chem. Rev. 114, 7421–7441.
Zhao, X.M., Zhou, S.W., Jiang, L.P., Hou, W.H., Shen, Q.M., Zhu, J.J., 2012. Chem. Eur J. 18, 4974–4981.
Zheng, H.Q., Zhang, Y.N., Liu, L.F., Wan, W., Guo, P., Nystrom, A.M., Zou, X.D., 2016. J. Am. Chem. Soc. 138, 962–968.
Zhou, H., Han, T.Q., Wei, Q., Zhang, S.S., 2016. Anal. Chem. 88, 2976–2983.
Zhou, Y.L., Xu, Z.N., Wang, M., Sun, B., Yin, H.S., Ai, S.Y., 2014. Biosens. Bioelectron. 53, 263–267.
Zhu, Q.Q., Zhuang, W., Chen, Y., Wang, Z.K., Hernandez, B.V., Wu, J.L., Yang, P.P., Liu, D., Zhu, C.J., Ying, H.J., Zhu, Z.H., 2018. ACS Appl. Mater. Interfaces 10, 16066–16076.
Zou, J.P., Wang, L.C., Luo, J., Nie, Y.C., Xing, Q.J., Luo, X.B., Du, H.M., Luo, S.L., Suib, S. L., 2016. Appl. Catal. B Environ. 193, 103–109.